Exergetic optimization of vortex tubes using a thermodynamic model

Conference Paper · May 2021

CITATIONS
2

READS
147

4 authors:

Junior Lagrandeur
Université de Sherbrooke
26 PUBLICATIONS **156** CITATIONS
SEE PROFILE

Sergio D. Croquer
Université de Sherbrooke
57 PUBLICATIONS **410** CITATIONS
SEE PROFILE

Sébastien Poncet
Université de Sherbrooke
414 PUBLICATIONS **3,912** CITATIONS
SEE PROFILE

Mikhail Sorin
Université de Sherbrooke
139 PUBLICATIONS **2,132** CITATIONS
SEE PROFILE

Exergetic optimization of vortex tubes using a thermodynamic model

Junior LAGRANDEUR[1]*, Sergio CROQUER[1], Sébastien PONCET[1] and Mikhail SORIN[1]

[1]Université de Sherbrooke,
Sherbrooke, Québec, Canada
Junior.Lagrandeur@USherbrooke.ca

* Corresponding Author

ABSTRACT

This article identifies sources of exergy losses in a vortex tube working with air by using a recently developed thermodynamic model and a reference experiment from the literature. Exergetic efficiency considering transiting exergy is used as the efficiency metrics in this work. When both the cold and hot outlets are useful, the exergetic efficiency reaches its maximum value for a cold mass fraction equal to 0.7. Interestingly, up to 45% of the inlet exergy is lost downstream of the vortex tube under this condition because of pressure losses in the cold tube and through measuring instruments. These losses do not contribute to the energy separation mechanism. Inside the vortex tube, the exergy irreversibly is mainly caused by the dissipation of kinetic exergy.

The thermodynamic model is also used to identify the working conditions, which maximize the vortex tube efficiency. The efficiency is always at its maximum value when the inlet Mach number is equal to one. The optimum value of the cold outlet diameter, the mass fraction and the cold outlet axial Mach number changes depending on whether thermal exergy from both outlets can be used or not. Increasing the cold outlet pressure increases the exergetic efficiency as well as changing the optimal condition for all variables except the inlet Mach number. At the end, the optimal vortex tube is twice as efficient as the reference vortex tube.

Finally, the model is employed to identify the best vortex tubes' arrangement to maximize the exergetic efficiency for an open cycle with a fixed inlet pressure of six bar. This analysis demonstrates that the best arrangement is a cascade of vortex tubes, where a vortex tube unit with the maximum efficiency is placed first. Two other vortex tubes are two other vortex tubes are placed to recover waste pressure on the cold and hot streams from the first unit.

1. INTRODUCTION

Vortex tubes generate a cold stream and a hot stream from a gas at neutral temperature. In a counterflow vortex tube, often called a Ranque-Hilsch vortex tube, a gas at neutral temperature is injected tangentially to generate a strong swirling flow. As shown in Figure 1, the gas is removed from two outlets: one on the axis near the injection point and one at the periphery at the other end of the tube.

Vortex tubes are cheap, reliable and they often used air as the working gas. In a recent review, Zhang and Guo (2018) listed all the many current and prospective applications of vortex tubes. However, their use is limited by their low efficiency. The authors attributed it to a lack of knowledge about the working mechanism inside the tube.

Xue *et al.* (2010) reviewed the energy transfer mechanism proposed since the invention of the vortex tube in the 1930's. They regrouped these explanations in six categories: pressure gradient, acoustic streaming, viscosity and turbulence, secondary circulation and static temperature gradient. However, none of them reaches a widespread acceptance because all these theories failed to predict the vortex tube performance (Lagrandeur *et al.* 2019a).

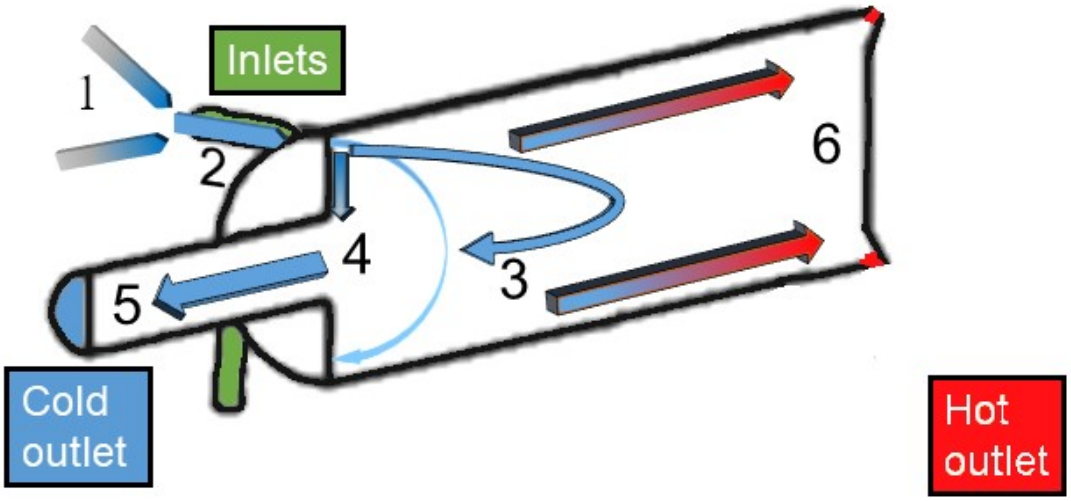

Figure 1: Illustration of the flow process in a vortex tube according the energy separation process used in the thermodynamic model. Figure adapted from Lagrandeur *et al.* (2020)

Recently, Lagrandeur *et al.* (2019b) described the flow process inside a vortex tube and used this description to create a thermodynamic model to predict the cold outlet temperature of vortex tubes. The flow process describe by this model used six steps (illustrated in Figure 1):

1. Gas is introduced at a given total inlet pressure (P_{0in}) and total inlet temperature (T_{0in}).
2. The gas accelerates in inlet nozzles to reach near sonic conditions. During the process, part of its thermal energy is converted into kinetic energy. The gas cools then down.
3. The gas swirls down the tube along the wall and part of it goes back to the middle of the tube towards the cold outlet. The flow is similar to a counterflow heat exchanger with flow in the center transferring energy to the flow at the periphery. The gas coming back to the entrance is then cooled at the same static temperature as the inlet, but with less kinetic energy because the rotation is slower near the axis.
4. The gas coming back from the tube is mixed with the Bödewadt boundary layer along the inlet plane, which has the same total temperature as the inlet.
5. Gas slows down as it goes down the cold tube, converting its kinetic energy to thermal energy.
6. Part of the gas goes out through the hot outlet with the energy removed from the cold stream.

The model reached a good qualitative and quantitative agreement when compared with the experimental data of Camiré (1995) and Skye *et al.* (2006) when friction losses are included in the model. This model includes most of the significant parameters identified by an artificial neural network (ANN) model (Lagrandeur *et al.* 2019b) with the exception of the vortex tube length. It is used to optimize the geometry and the working conditions of a single vortex tube in this article.

Another way to improve the efficiency is to combine multiple vortex tubes in cascades. Dincer (2011) and Dincer *et al.* (2011) demonstrated that using vortex tubes in hot cascade configuration increases the temperature difference between both outlets and the exergetic efficiency compared to a single vortex tube. Attala *et al.* (2017) compared the cold cascade, the hot cascade and parallel vortex tubes and found that the cold cascade increases the cold outlet temperature drop and the cooling *COP* (coefficient of performance), but reduce the heating COP and the hot outlet temperature rise. Shmroukh *et al. (2019)* compared the parallel, the cold cascade and the hot cascade arrangements on a seawater desalination system and found that the system using the hot cascade can treat more water over a 3-hour period. Finally, Majidi *et al.* (2018) used a modified version of the model of Ahlborn *et al.* (1994) to simulate vortex tube cascades. However, this model is inconsistent with the treatment of kinetic energy and compressibility (Gao, 2005). Authors believed this model would fail for the high pressures considered in the present paper.

This paper will present the optimization of a single vortex tube and vortex tubes cascades using the thermodynamic model previously developed. The exergy efficiency considering exergy in transit (Brodyansky *et al.,* 1994; Sorin and Khennich, 2018) is selected as the performance metric. The exergetic efficiency of a single tube is analyzed, and sources of exergy losses at each step are identified. Finally, the optimal vortex tube cascade is proposed.

2. RESULTS

2.1 Exergetic Efficiency Definition

The common definition of exergetic efficiency (Grassmann efficiency) is just the ratio of the total outlet exergy to the total inlet exergy. However, this definition includes in the numerator and the denominator exergy that goes through the system without any change. For example, in the vortex tube, leftover pressure could increase the efficiency artificially.

To solve this problem, Brodyansky *et al.* (1994) removed the transiting exergy from the numerator and the denominator. For a vortex tube, the efficiency is calculated using:

$$\eta_{vt} = \frac{\mu_c \Delta e_T^{in-c} + (1-\mu_c)\Delta e_T^{in-h}}{\mu_c \nabla e_P^{in-c} + (1-\mu_c)\nabla e_P^{in-h}}, \tag{1}$$

where η_{vt} is the exergetic efficiency considering the transiting exergy, μ_c is the cold mass fraction, Δe_T^{in-x} is the thermal exergy generated between the inlet and the cold outlet (c) or the hot outlet (h) and ∇e_P^{in-x} is the mechanical exergy consumed between the inlet and the specified outlet. These terms are calculated using:

$$\Delta e_T^{in-c} = \left[\left(T_{0c} - T_{0in} \right) - T_{ref} C_p \left(T_{0c} / T_{0in} \right) \right], \tag{2}$$

$$\Delta e_T^{in-h} = \left[\left(T_{0h} - T_{0in} \right) - T_{ref} C_p \left(T_{0h} / T_{0in} \right) \right], \tag{3}$$

$$\nabla e_P^{in-c} = R \ln \left(P_{0in} / \overline{P}_c \right), \tag{4}$$

$$\nabla e_P^{in-h} = R \ln \left(P_{0in} / \overline{P}_h \right), \tag{5}$$

with T_0 the total temperature, T_{ref} the reference temperature, P_0, the total pressure, $\overline{P}$ the mean static pressure, R the specific perfect gas constant and C_p the specific heat at constant pressure. If the vortex tube is replaced in a system, mechanical exergy consumption upstream and downstream of the vortex tube can be calculated in a similar way. Details about their calculation are given in Lagrandeur *et al.* (2020) along with the calculations of T_{0h} and mean outlet static pressure. Calculation of T_{0c} is done using the thermodynamic model.

2.2 Exergy Transformation in Vortex tube

The thermodynamic model separates the energy transfer process in the vortex tube in multiple steps. As a consequence, it is possible to evaluate how exergy is transformed or consumed in the vortex tube. Table 1 presents the specific exergy at each step presented in Figure 1 for a reference case at μ_c=0.63 and P_{0in}=3.08 bar. These conditions correspond to the maximum energy separation from the experimental data of Camiré (1995). Exergy generated and consumed at other experimental conditions can be found in Lagrandeur *et al.* (2020). The exergy flow is also illustrated on the Grassmann diagram of Figure 2.

Table 1: Specific exergy (kJ kg^{-1}) at different steps of the energy separation process inside the vortex tube.

#	STEP	TOTAL	MECH.	THER.	KIN.
1	Stagnation	95.1	95.1	0	0
2	Acceleration with friction	90.3	59.8	1.5	29.0
3	Cold flow to center	35.0	29.3	1.5	4.2
4	Mixing with the boundary layer	34.7	29.3	1.2	4.2
5	Cold outlet	30.1	29.3	0.8	0
6	Hot outlet	44.8	42.6	2.2	0

One could observe that the thermal exergy generated is small compared to the available mechanical exergy. However, one could observe too that only 37% of the available exergy is consumed by the energy separation process. In fact, a large share of the inlet mechanical exergy is lost through pressure drops outside of the vortex tube in the inlet nozzles or downstream of both outlets (leftover pressure). Since air in this experiment is going to the

atmosphere, any leftover mechanical exergy is lost. As a consequence, minimizing pressure drops upstream or downstream of the vortex tube would improve greatly its efficiency.

Inside the vortex tube, another source of losses is by kinetic exergy destruction. Almost half of the exergy consumed between step 2 and both outlets is from kinetic exergy destruction. Part of it is unavoidable because the tangential velocity gradient is used to generate the temperature difference (between steps 2 and 3). However, part of the kinetic exergy going downstream in the tube (steps 2 to 6) or going out of the cold outlet (steps 4 to 5) may be converted to mechanical exergy using diffuser. This mechanism may explain the best performance obtained with conical vortex tube (Yilmaz *et al.*, 2009) or with a vortex tube equipped with a diffuser in the cold tube (Farzaneh-Gord and Sadi, 2014). Another alternative is the double-circuit vortex tube (Rafiee and Sadeghiazad, 2017). In this case, an additional flow appears on the axis at the hot end. This flow is cooled down at the same temperature as the rest, but it does not consume tangential kinetic exergy in the process.

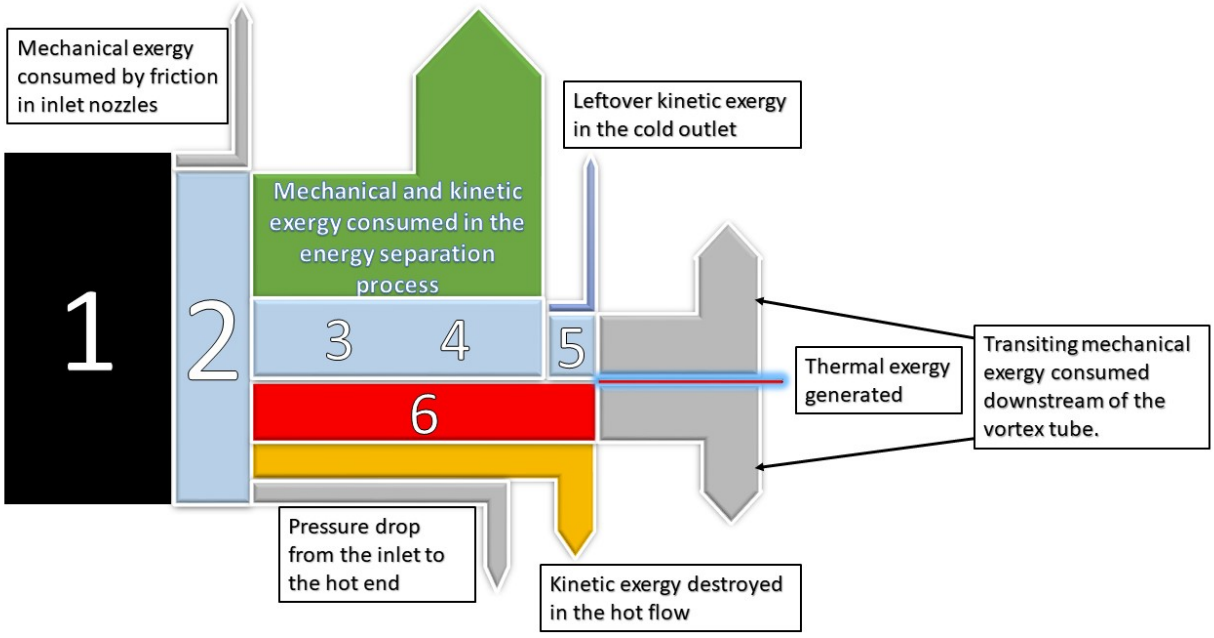

Figure 2: Grassmann diagram of the exergy flow in the vortex tube at each step illustrated in Figure 1 and detailed in Table 1. Figure adapted from Lagrandeur *et al.* (2020).

2.3 Parametric Optimization of the Single Vortex Tube

The thermodynamic model is used to optimize four operational and geometrical parameters of the vortex tube:

- Inlet Mach number (Ma_{in}) ranging from 0.5 to 1;
- μ_c ranging from 0.1 to 0.9;
- Ratio of cold outlet radius to vortex tube radius (r_c/r_{vt}) ranging from 0.1 to 0.7;
- the axial Mach number in the cold outlet Ma_{zc}, ranging from 0.05 to 0.7.

For each of these parameters, eleven different values are tested for two different mean cold outlet pressures: 1 bar and 3 bar. The inlet temperature is set to 295 K for all cases. In addition to the global exergetic efficiency defined in Equation (1), some other performance metrics are investigated: lowest T_{0c}, highest specific cooling power (q_c) and exergetic efficiency calculated using Equation (1), but with only the cold part or the hot part of the numerator (η_c and η_h). Results of these calculations are presented in Tables 2 and 3.

Table 2: Optimum working conditions of the vortex tube for a mean cold outlet pressure of 1 bar

	Ma_{in}	μ_c	r_c/r_{vt}	Ma_z	T_{0c} (K)	T_{0h} (K)	P_h (bar)	Q_c (kJ/kg)	η_c (%)	η_h (%)	η_{vt} (%)
MIN T_{0C}	1	0.26	0.34	0.18	254.6	309.2	1.27	10.6	0.8	0.3	1.1
MAX Q_C	1	0.66	0.52	0.31	261.0	361.0	1.57	22.6	1.5	2.4	3.9
MAX η_C	1	0.58	0.46	0.25	257.2	347.2	1.80	22.1	1.8	2.0	3.8
MAX η_H	1	0.74	0.64	0.25	265.2	379.8	1.66	22.2	1.4	3.0	4.4
MAX η_{VT}	1	0.74	0.64	0.25	265.2	379.8	1.66	22.2	1.4	3.0	4.4

Table 3: Optimum working conditions of the vortex tube for a mean cold outlet pressure of 3 bar

	Ma_{in}	μ_c	r_c/r_{vt}	Ma_z	T_{0c} (K)	T_{0h} (K)	P_h (bar)	Q_c (kJ/kg)	η_c (%)	η_h (%)	η_{vt} (%)
MIN T_{0C}	1	0.42	0.28	0.18	252.7	325.6	3.96	17.9	1.5	0.9	2.4
MAX Q_C	1	0.74	0.4	0.25	259.8	395.1	5.19	26.2	1.8	3.8	5.6
MAX η_C	1	0.58	0.28	0.25	254.2	351.4	5.40	23.9	2.01	2.3	4.3
MAX η_H	0.95	0.82	0.52	0.18	269.2	412.4	5.12	21.3	1.1	3.9	5.0
MAX η_{VT}	1	0.74	0.46	0.18	260.0	394.7	5.15	26.1	1.8	3.8	5.6

The first observation from these two tables is that performance increases for all metrics when the cold outlet pressure increases. This is quite interesting since the effect of the cold outlet pressure has not been studied experimentally or numerically yet. Another observation is that the optimal parameters differ widely depending on the objective and on the outlet pressure. Higher cold outlet pressure promotes a smaller cold outlet radius and higher values of μ_c. For Ma_z, having a higher cold outlet pressure reduces the optimal axial Mach number. With a higher air density at the outlet with a higher pressure, it may indicate a possible optimal mass flow rate through the cold outlet.

For the inlet Mach number, with one exception, the optimal value is always at the maximum sonic value. In consequence, the stronger the velocity gradient between the center and the periphery, the higher the temperature separation. Supersonic shock wave has not been investigated yet. It could improve the performance if sudden expansion and shock wave do not affect the shape of the vortex.

Finally, optimal values identified for T_{0c} and q_c for an outlet to the atmosphere are in accordance with values from the literature as summarized in Lagrandeur *et al.* (2019b). For the exergetic efficiency, one comparison is with the experimental data of Camiré (1995). The exergetic efficiency of the vortex tube obtained with the optimization process is almost twice the maximum value obtained from the experiment. It highlights the potential of this technique to significantly increase the efficiency of vortex tubes.

2.4 Optimal Vortex Tubes Combination at a Fixed Inlet Pressure

As a final step, the thermodynamic model is used to identify the best vortex tube combination for a fixed inlet pressure of 6 bar, typical of industrial compress air systems, and a mean outlet pressure of 1 atm. The performance metric considered in this section is the exergetic efficiency when both outlets are considered useful. However, leftover pressure is wasted in this case and multiple vortex tubes could generate thermal exergy. As consequence, a new exergy efficiency definition is proposed:

$$\eta_{cas} = \frac{\Delta e_T^{vt1} + \Delta e_T^{vt2}}{e_{in}}, \tag{6}$$

with η_{cas} the exergetic efficiency of the cascade, e_{in} the total mechanical exergy available at the inlet of the first vortex tube and Δe_T^{vt} the total thermal exergy generated in each vortex tube.

According to the thermodynamic model, Ma_{in} and P_{0in} are related by this equation (Lagrandeur *et al.*, 2019b):

$$\frac{P_{0in}}{P_c} = \left(1 + \frac{\gamma - 1}{2} \mathrm{Ma}_{in}^2\right)^{\gamma/(\gamma-1)} \exp\left(\frac{\gamma}{2} \mathrm{Ma}_{in}^2\right), \tag{7}$$

with γ the specific heat ratio of the gas. Because this equation is implicit for the Mach number but not for the inlet pressure, different Mach numbers are tested and cases with P_{0in} over 6 bar are discarded.
Additionally, with a pressure ratio P_{0in}/P_c equal to 6, Mach number is always greater than one. It is then necessary to reduce this pressure ratio by reducing the inlet pressure or by increasing the cold outlet pressure. To identify the most favorable condition between these two possibilities, different cold outlet pressures are tested in this analysis.
The best single vortex tube (SVT) is detailed in Table 4. As illustrated, it is preferable to raise the cold outlet pressure than to reduce the inlet pressure to maximize the efficiency of a single vortex tube fed by excessive pressure. These results confirm the beneficial impact of a higher cold outlet pressure highlighted in the previous section.

Table 4: Optimal vortex tubes combinations with a fixed inlet pressure of 6 bar

	Ma_{in}	μ_c	r_c/r_{vt}	Ma_z	T_{0c} (K)	T_{0h} (K)	P_{0in} (bar)	$\bar{P}_c$ (bar)	P_h (bar)	η_{vt} (%)	η_{cas} (%)
SVT	1	0.74	0.52	0.25	262	388	5.9	1.7	2.8	5.0	3.1
CC	0.65	0.74	0.58	0.12	249	299	1.7	1.0	1.3	2.4	3.6
HC1	0.9	0.66	0.52	0.25	350	461	2.8	1.0	1.6	3.6	3.6
HC2	0.6	0.74	0.52	0.18	442	515	1.6	1.0	1.2	1.9	3.6

From the SVT results, one may observe that there is pressure available for a second vortex tube at both inlets. To get the optimal performance, it is better to maximize the efficiency of the first vortex tube (Lagrandeur *et al.*, 2020). Consequently, the SVT is used to feed another vortex tube in the cold cascade (CC) and hot cascade (HC) configurations.

There is more pressure available on the hot side than on the cold side of the first vortex tube. η_{vt} is then higher for HC1 than for CC. However, because of the high cold mass fraction in SVT, the impact of both cascades remains the same on η_{cas}. If both cascades are combined, $\eta_{cas} = 4.0$.

At the hot outlet of HC1, there is still a significant pressure available at the hot outlet. It is possible to install another vortex tube in a hot cascade arrangement. However, because only 8.9% of the inlet flow is sent to the last tube, the effect on η_{cas} is negligible.

2.4 Combining Vortex Tubes with an Ejector

The cold cascade configuration is interesting to maximize the generation of cold thermal exergy. However, there is less pressure available on the cold side than on the hot side. To maximize the efficiency of the second vortex tube, it is proposed to use an ejector to increase the pressure of the cold stream using the higher pressure of the hot stream.

The proposed configuration is shown in Figure 3. In this system, the hot stream is cooled to atmospheric condition in a heat exchanger. Pressure losses in the heat exchanger are neglected. The stream is then injected as the primary stream in the ejector. The cold stream of the first vortex tube is the secondary stream. Both streams mix in the ejector, and the pressure at the ejector outlet is higher to the pressure of the cold stream. This cold stream is then sent to a second vortex tube.

To model the ejector, the thermodynamic model proposed by Croquer *et al.* (2017) is used. This model calculates the outlet temperature and pressure of an optimal ejector using the inlet condition of both streams. However, experimental data about ejectors are limited to entrainment ratio under one. As a consequence, the cold mass fraction of the first vortex tube must be limited to 0.5, which is not the most efficient configuration for the first vortex tube.

When increasing the cold mass fraction of the first vortex tube, the cold outlet pressure stays constant at 1.6 bar, but the hot outlet pressure rises from 2.5 to 3.0 bar. Consequently, the primary pressure available to compress the cold stream rises. At the same time, the ejector outlet pressure reduces when the entrainment ratio goes up. Both effects balance in this case and the ejector outlet pressure varies between 2.0 and 2.3 bar for a cold mass fraction between 0.15 and 0.5. The configuration with the lowest ejector outlet temperature is the most interesting. This configuration is obtained for a cold mass fraction of 0.5 in the first vortex tube, corresponding to an entrainment ratio of one.

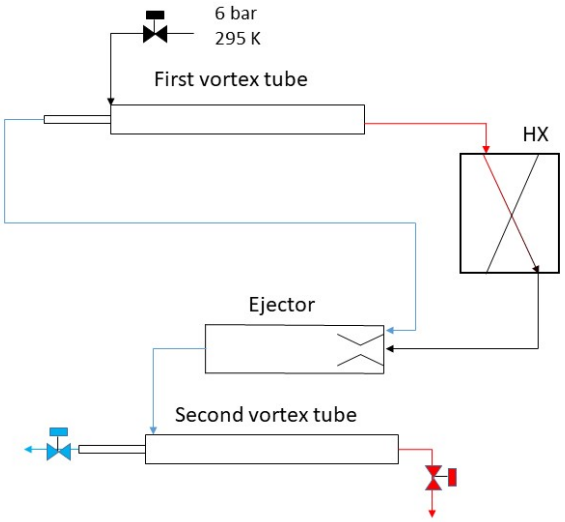

Figure 3: Proposed cold cascade with an ejector between both tubes

For the second vortex tube, the increase in performance due to higher inlet pressure does not compensate for the loss in performance of the first vortex tube working under its optimal cold mass fraction. This configuration generates less cold outlet thermal exergy than the CC configuration. However, this configuration increases the cooling power (q_c=26.1 kJ.kg^{-1}) when compared to the SVT (q_c=24.6 kJ.kg^{-1}) and the CC (q_c=25.4 kJ.kg^{-1}). However, it is not enough to justify the added complexity of the system.

3. CONCLUSION

The work demonstrated that it is possible to increase significantly the performance of the vortex tube by using a validated thermodynamic model. Advantages of using a thermodynamic model are the insight provided by a deeper understanding of the energy separation process and the ability to test a huge number of combinations in a short amount of time.

Below are the main highlights of this work:

- Exergy efficiency considering transiting exergy is used as the performance metric.
- Exergetic efficiency is increased from 2.9% (maximum efficiency from the reference experiment) to 4.4% for the optimized vortex tube modeled using the thermodynamic model. The improvement is achieved by increasing the radius of the cold outlet and increasing the mass flow at the inlet.
- Up to 51% of the mechanical exergy available at the inlet is consumed upstream or downstream of the vortex tube through pressure losses in the reference experiment.
- Mostly kinetic exergy is consumed in the energy separation process.
- Optimum working conditions and geometry of the vortex tube depend strongly on the chosen performance metric.
- Increasing the cold outlet pressure increases the exergetic efficiency of the vortex tube (4.4% to 5.6%).
- For a pressure fixed to 6 bar at the inlet and an outlet at the atmosphere, using vortex tubes in a hot and cold cascade configuration increases the exergy efficiency of the system from 3.1% to 4%.
- Using an ejector between the first and the second vortex tubes in a cold cascade configuration did not improve the exergetic efficiency.
- Future work could validate experimentally the optimal working conditions obtained from the model. Additionally, there is a need to further explore the effect of the cold outlet pressure on the performance of vortex tubes.

NOMENCLATURE

The nomenclature should be located at the end of the text using the following format:

Cp	specific heat at constant pressure	($J.kg^{-1}.K^{-1}$)
Ma	Mach number	(-)
P, $\overline{P}$, P_0	static pressure, mean static pressure and total pressure	(bar)
R	specific perfect gas constant	($J.kg^{-1}.K^{-1}$)
T, T_0	static and total temperature	(K)
∇e_P	mechanical exergy consumed	($kJ.kg^{-1}$)
Δe_T	thermal exergy generation	($kJ.kg^{-1}$)
γ	specific heat ratio	(-)
η	exergetic efficiency	(-)
μ_c	cold mass fraction	(-)

Subscript

c	cold outlet
cas	cascade
h	hot outlet
in	inlet
vt	vortex tube
z	axial through the cold outlet

REFERENCES

Ahlborn, B., Keller, J. U., Staudt, R., Treitz, G., & Rebhan, E. (1994). Limits of temperature separation in a vortex tube. *Journal of Physics D: Applied Physics*, 27(3), 480-488.

Attalla, M., Ahmed, H., Ahmed, M. S., & El-Wafa, A. A. (2017). Experimental investigation for thermal performance of series and parallel Ranque-Hilsch vortex tube systems. *Applied Thermal Engineering*, 123, 327–339.

Brodyansky, Sorin, M. V., & Le Goff, P. (1994). *The efficiency of industrial processes*: E*xergy analysis and optimization.* Amsterdam, The Netherlands: Elsevier.

Camiré, J. (1995). Experimental investigation of vortex tube concepts, Master thesis, University of British Columbia, 130 p.

Croquer, S., Poncet, S., & Aidoun, Z. (2017). Thermodynamic modelling of supersonic gas ejector with droplets. *Entropy*, 19(11), 579.

Dincer, K. (2011). Experimental investigation of the effects of threefold type Ranque–Hilsch vortex tube and six cascade type Ranque–Hilsch vortex tube on the performance of counter flow Ranque–Hilsch vortex tubes. *International Journal of Refrigeration*, 34(6), 1366–1371.

Dincer, K., Yilmaz, Y., Berber, A., & Baskaya, S. (2011). Experimental investigation of performance of hot cascade type Ranque–Hilsch vortex tube and exergy analysis. *International Journal of Refrigeration*, 34(4), 1117–1124.

Farzaneh-Gord, M., & Sadi, M. (2014). Improving vortex tube performance based on vortex generator design. *Energy*, 72, 492–500.

Gao, C. (2005). Experimental study on the Ranque-Hilsch vortex tube. Ph.D. thesis, Technische Universiteit Eindhoven, The Netherlands 151 p.

Lagrandeur, J., Poncet, S., & Sorin, M. (2019a). Review of predictive models for the design of counterflow vortex tubes working with perfect gas*. International Journal of Thermal Sciences*, 142, 188–204.

Lagrandeur, J., Poncet, S., Sorin, M., & Khennich, M. (2019b). Thermodynamic modeling and artificial neural network of air counterflow vortex tubes. *International Journal of Thermal Sciences*, 146, 106097.

Lagrandeur, J., Croquer, S., Poncet, S., & Sorin, M. (2020). Exergy analysis of the flow process and exergetic optimization of counterflow vortex tubes working with air. *International Journal of Heat and Mass Transfer*, 152, 119527.

Majidi, D., Alighardashi, H., & Farhadi, F. (2018). Best vortex tube cascade for highest thermal separation. *International Journal of Refrigeration*, 85, 282–291.

Rafiee, S. E., & Sadeghiazad, M. M. (2017). Improving the energetical performance of vortex tubes based on a comparison between parallel, Ranque-Hilsch and Double-Circuit vortex tubes using both experimental and CFD approaches. *Applied Thermal Engineering*, 123, 1223–1236.

Shmroukh, A. N., Radwan, A., Abdal-hay, A., Serageldin, A. A., & Nasr, M. (2019). New configurations for sea water desalination system using Ranque-Hilsch vortex tubes. *Applied Thermal Engineering*, 157, 113757.

Skye, H. M., Nellis, G. F., & Klein, S. A. (2006). Comparison of CFD analysis to empirical data in a commercial vortex tube. *International Journal of Refrigeration*, 29(1), 71–80.

Sorin, M., & Khennich, M. (2018). *Exergy Flows Inside Expansion and Compression Devices Operating below and across Ambient Temperature*. In. P. Tsvetkov, *Energy Systems and Environment*, (61–82), London, UK: IntechOpen.

Xue, Y., Arjomandi, M., & Kelso, R. (2010). A critical review of temperature separation in a vortex tube. *Experimental Thermal and Fluid Science*, 34(8), 1367–1374.

Yilmaz, M., Kaya, Karagoz, S., & Erdogan, S. (2009). A review on design criteria for vortex tubes. *Heat and Mass Transfer*, 45(5), 613–632.

Zhang, B., & Guo, X. (2018). Prospective applications of Ranque–Hilsch vortex tubes to sustainable energy utilization and energy efficiency improvement with energy and mass separation. *Renewable and Sustainable Energy Reviews*, 89, 135–150.

ACKNOWLEDGEMENT

This work is funded by the Natural Sciences and Engineering Research Council of Canada (NSERC) [ESD2-502366-2017] and by the *Fond de Recherche du Québec – Nature et Technologies* (FRQNT) [255888]. Authors would like to acknowledge the support of the NSERC chair on industrial energy efficiency established at the University of Sherbrooke in 2019 with the contribution of Hydro-Québec, Natural Resources Canada and Emerson.